Nuclear Instruments and Methods in Physics Research A ▮ (▮▮▮▮) ▮▮▮–▮▮▮

Contents lists available at ScienceDirect

Nuclear Instruments and Methods in Physics Research A

journal homepage: www.elsevier.com/locate/nima

A very high performance stabilization system for large mass bolometer experiments

C. Arnaboldi [a,b], A. Giachero [a,b,*], C. Gotti [a,c], G. Pessina [a,b]

[a] Sezione INFN di Milano Bicocca, Piazza della Scienza 3, I-20126 Milano, Italy
[b] Università di Milano Bicocca, Piazza della Scienza 3, I-20126 Milano, Italy
[c] Universitá di Firenze, Dipartimento di Elettronica e Telecomunicazioni, Via S. Marta 3, I-50139 Firenze, Italy

ARTICLE INFO

Keywords:
Double beta decay
Bolometers
CUORE
Response stabilization
Optical coupling

ABSTRACT

CUORE is a large mass bolometric experiment, composed of 988 crystals, under construction in Hall A of the Gran Sasso Underground Laboratories (LNGS). Its main aim is the study of neutrinoless double beta decay of ^{130}Te. Each bolometer is a 760 g crystal of Tellurium dioxide on which a Nuclear Transmutation Doped Ge thermistor, Ge NTD, is glued with proper thermal contact. The stability of the system is mandatory over many years of data taking. To accomplish this requirement a heating resistor is glued on each detector across which a voltage pulse can be injected at will, to develop a known calibrated heating power. We present the design solution for a pulse generator system to be used for the injection of such a small and short voltage pulse across the heaters. This system is composed by different custom PCB boards each of them having multi-channel independent outputs completely remotely programmable from the acquisition system, in pulse width and amplitude, through an on-board ARM7 microcontroller. Pulse amplitudes must be selectable, in order to handle each detector on its full dynamic range. The resolution of the output voltage is 12 bits over 10 V range. An additional 4 steps programmable voltage attenuator is added at every output. The width of any pulse can range from 100 μs to 25.5 ms. The main features of the final system are: stability and precision in pulses generation (at the level of less than a ppm/°C), low cost (thanks to the use of commercial components) and compact implementation.

1. Introduction

CUORE [1] is a large mass bolometric experiment that will be placed in the hall A of the Gran Sasso Underground Laboratory (LNGS). Its main aim is the search for neutrinoless double beta decay, a very important topic in the field of neutrino physics since the discovery of neutrino oscillations. In fact, by studying this rare nuclear transition it is possible to prove the Majorana nature of neutrinos and to obtain information on the their mass hierarchy and scale. The chosen nucleus, as source of the decay, is the ^{130}Te isotope present in natural TeO_2 crystals, $5\times5\times5\ cm^3$ (760 g) each [1]. These crystals work also as bolometer absorbers, by converting the energy released by any impinging particle into a temperature increase, that is readout by a thermistor glued on them. Measurable temperature variations can be obtained working at very low temperatures ($T_0 \simeq 10$ mK). The entire detector will consist of an array of 988 TeO_2 bolometers (750 Kg of total mass) arranged in a cylindrical configuration composed of 19 towers. Each tower will have four columns and each column will be composed of 13 crystals.

2. Stabilization technique

To maintain the temperature around 10 mK a bolometric experiment, like CUORE, needs a proper cryogenic setup. Unfortunately this kind of systems shows intrinsic instabilities which can spoil the energy conversion gain and the energy resolution. Since the experiment must take data for a long time without human intervention, it is mandatory to develop a system to stabilize the detector response or, at least, to correct its instabilities. The experience gained in previous bolometric experiments, such as CUORICINO [2] and Milano-DBD [3], shows that a way to accomplish this goal is to periodically deliver to the detector one or more fixed amounts of energy inducing a detector response as similar as possible to the ones generated by the events of interest [4]. This technique allows to monitor the pulse amplitude variations and, off-line, to correlate these variations with the detector baseline drifts and, then, to stabilizate the

* Corresponding author at: Sezione INFN di Milano Bicocca, Piazza della Scienza 3, I-20126 Milano, Italy. Tel.: +39 02 6448 2456; fax: +39 02 6448 2463.
E-mail address: Andrea.Giachero@mib.infn.it (A. Giachero).

0168-9002/$ - see front matter © 2010 Elsevier B.V. All rights reserved.
doi:10.1016/j.nima.2010.09.151

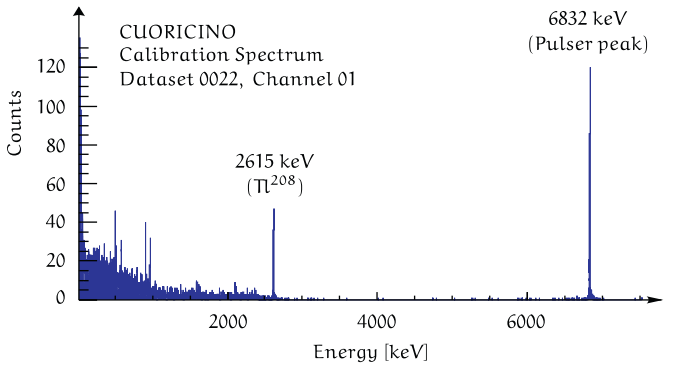

Fig. 1. Example of calibration spectrum for channel 1 of the CUORICINO experiment. The 6832 keV line is due to the stabilization heater pulses while the other lines are generated from the particle calibration source.

energy conversion gain. The fixed energy injection into the bolometer can be realized in two ways:

1. *mono-energetic particle absorption* exploiting a radioactive source. The advantage of this solution is that the detector response is identical (or very similar) to the response to the events of interest. The disadvantage is that a natural source of energetic particles left close to the measurement apparatus, would increase the radioactive background. This method is typically used to periodically calibrate the detector, but the radioactive source is removed during the normal data taking;
2. *Joule pulses* delivered by a heating resistor, thermally coupled to the crystal. The advantage of this solution is the complete control of the pulse generation procedure. The generated pulse rate and amplitude can be tuned. The relationship between the joule power delivered and the energy measured depends on the thermal coupling between the heating resistor and the crystal. For this reason this method cannot be an absolute reference and needs an initial calibration. Nevertheless a very accurate stabilization can be achieved.

The adopted solution is mixed: the radioactive source is used to calibrate the system (in the case of CUORICINO the detector was calibrated approximately once per month by the insertion of thoriated tungsten wires on opposite sides of the cryostat), while the heating source is used to stabilize it.

The *stabilization heater pulses* are provided by a voltage signal developed across a resistive heater glued on the bolometer crystal. The heater pulses are used to monitor the gain and establish its dependence on temperature. The gain stabilization procedure consists of fitting the heater pulse amplitude as a function of the detector baseline. After this procedure the responses of the bolometers are rescaled to the initial calibration values. In this way the energy resolution is maintained at its optimum value for the entire data taking between calibrations. A typical spectrum produced after the stabilization and calibration procedures is shown in Fig. 1.

3. Stabilization system: the pulser

Heater pulses are generated by a custom calibration system. In this paper we present the first four-channel prototype, and its characterization. The instrument, an upgrade of the solution used in the CUORICINO experiment [5], is a programmable pulse generator (*pulser*) that consists of a board having multichannel independent outputs, completely remotely programmable from the acquisition and control system. An on-board ARM7 (LPC2378) microcontroller configures the pulse width (t_w), the pulse amplitudes (V_g) and the pulse trigger. The remote control is performed through a message based CAN-Bus protocol optically coupled to the board. The triggering of any pulse is fired by the acquisition system, to allow the tagging of all the calibrating pulses. The generated signals are square pulses, $\delta(t)$-like, having a width much shorter than the detector signal. The amplitudes are selectable, thanks to an on-board DAC (AD5415), in order to handle each detector on its full dynamic range. The DAC generates a current proportional to the selected value which is converted into a voltage by two external operational amplifiers, as shown in Fig. 6 (black circuit). The resolution of the output voltage is 12 bits across a 10 V range. An additional 4 step, differential, programmable voltage attenuator, not shown in Fig. 6, is added on every output. The width of pulses can range from 100 μs to 25.5 ms, with a resolution of 100 μs (8 bits), exploiting an on-board CPLD (Xilinx XCR3256XL) and an external clock generator. All the DACs, two per channel, and all the CPLDs, one every 4 channels, are controlled by the microcontroller through the SPI synchronous serial data bus. Care was taken to obtain a very precise width of the pulses. A special circuit is dedicated to correct the residual drift of the analog path, from the reference voltage to the differential output voltage of the pulser.

An *external clock generator board* is used to generate a precise time reference for the construction of the analog pulse width. This circuit is based on a crystal oscillator module working at 10 MHz. The oscillator has a specified frequency stability of 50 ppm over 0–70 °C temperature operating range (with a supply voltage of 5 ± 0.25 V). The communication between the CPLD and the clock-generator occurs through two optical lines: CK (*clock*) and CK_REQ (*clock request*).

The pulse generation procedure is as follows. The control system (hereafter CS) communicates the amplitude of the pulse and its width to the microcontroller for a selected channel. The microcontroller receives the command and configures the amplitude on the DAC and the pulse width on the CPLD. Finally the CS sends the trigger command in order to generate the pulse. All the commands are sent to the microcontroller via CAN-bus. When the CPLD receives the trigger command the clock request is enabled and, as consequence, the clock-generator sends the 10 MHz clock to the CPLD counter, through the CK line. Upon the first received clock pulse the CPLD enables the DAC output (LDAC, *Load DAC*, digital signal), and, when the number of received clock pulses equals the required pulse width, the CPLD disables the DAC output (CLR, *Clear DAC*, digital signal) and the calibration pulse is generated. During the generation of signals the ARM is maintained in idle condition to avoid possible interferences from its clock.

4. Pulse characterization

The energy released (E_{released}) to the bolometer depends on the energy provided by the pulse generator (E_{heater}). For a fixed value of heater resistance energy is given by:

$$E_{\text{heater}} = \frac{V_g^2}{R_{\text{heater}}} t_w \tag{1}$$

The conversion factor $E_{\text{released}} \leftrightarrow E_{\text{heater}}$ is not exactly computable in advance because of the unknown thermal coupling between the heater resistor and the crystal absorber. To measure it a calibration with a radiative source is needed.

Neglecting, at first approximation, the heater resistance contribution, the pulse error can be expressed as:

$$\frac{\Delta E_{\text{heater}}}{E_{\text{heater}}} = \frac{\Delta t_w}{t_w} + 2\frac{\Delta V_g}{V_g} \tag{2}$$

Please cite this article as: C. Arnaboldi, et al., Nucl. Instr. and Meth. A (2010), doi:10.1016/j.nima.2010.09.151

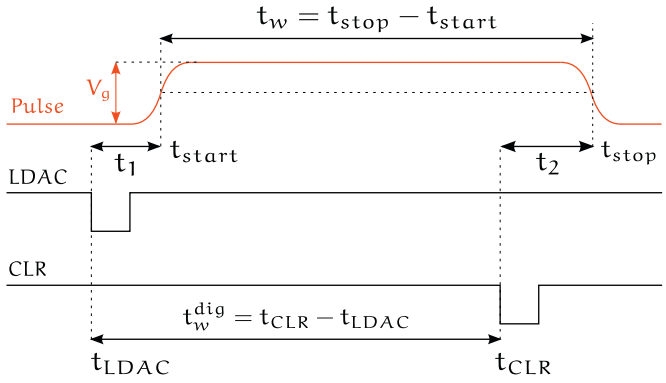

Fig. 2. Time diagram of signals involved in the pulse generation process. LDAC and CLR are the digital signal through which the CLPD drives the DAC output.

The goal is to minimize this error maintaining the stability and precision in pulses generation at the level of less than a ppm/°C. In order to check if the prototype satisfies this requirement we measured the temperature drift of t_w and v_g as a function of temperature. Temperatures were controlled by a Vötsch® VC4018 Environmental Chamber.

Considering first the pulse width and taking into account the time diagram shown in Fig. 2 one has:

$$\begin{cases} t_w = t_{stop} - t_{start} \\ t_w^{dig} = t_{CLR} - t_{LDAC} \end{cases} \Rightarrow t_w = t_{CLR} - t_{LDAC} - (t_1 - t_2) \quad (3)$$

And, at last, with the substitution $t_{12} = t_1 - t_2$:

$$t_w = t_w^{dig} - t_{12} \quad (4)$$

In this form the pulse width can be split into two different contributions: the former, t_w^{dig} is due to the digital parts of the system (CPLD and Clock generator) while the latter depends on its analog parts (DAC and Op-Amps). According to Eq. (4), the total temperature drift of the pulse width is given by:

$$\frac{\Delta t_w}{t_w}(T) = \frac{\Delta t_w^{dig}}{t_w}(T) - \frac{\Delta t_{12}}{t_w}(T) \quad (5)$$

The two instants t_1 and t_2 represent, respectively, the delays of the analog signal, evaluated at half maximum, from the start (LDAC) and the stop (CLR) triggers. These two delays are added by the analog parts. The output signal has a rise and a fall time respectively of around 160 and 120 ns, and an expected time jitter smaller than 200 ps_{RMS}. To get an accurate measurement of these parameters, avoiding the limitation in amplitude resolution of a fast 8-bits real time oscilloscope, we used a sampling oscilloscope (Agilent® 86100 DCA-J wideband, 40 Gb/s) having amplitude resolution of 14 bits, time resolution up to 2 ps/div and noise floor of only 0.2 mV_{RMS} when limited to 12 GHz analog bandwidth. We created a repetitive signal and, exploiting LDAC and CLR as digital triggers, we measured $t_{12} = t_1 - t_2$ in the range from 0 to 50 °C with steps of 5 °C. Results (Fig. 3) show a linear trend with $\Delta t_{12}/\Delta T = (0.200 \pm 0.005)$ns/°C slope.

The quantity t_w^{dig} is the time interval between the start (LDAC) and stop (CLR) signals. These are 3.3 V-CMOS standard signals with rise and fall times around 20 ns. This time we measured the trigger time-stamp of the widely separated time instants LDAC and CLR, with a time resolution of 50 ps/pt, using a Tektronix® DPO7254, 2.5 GHz, oscilloscope having 20 Mpoints/ch of memory depth. Computing, for every temperature step, the difference between the two time-stamps and fitting the resulting distribution with a Gaussian function we obtained the value of t_w^{dig} vs. T. This measurement was performed for three different pulse

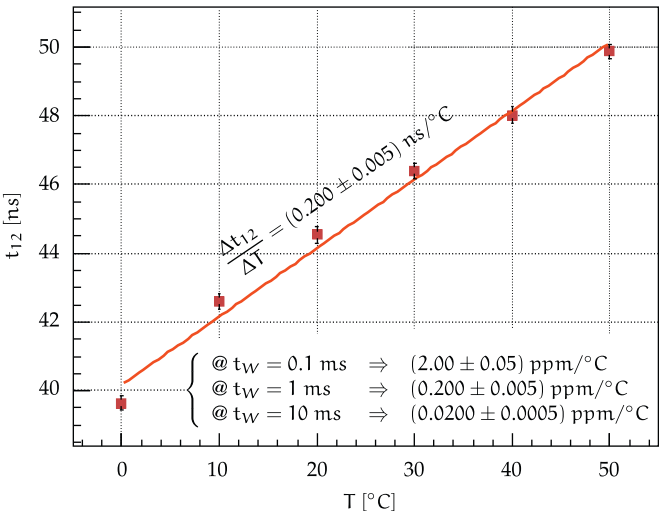

Fig. 3. Pulse width: example of temperature drift trend due to the analogs parts (DAC and Op-Amps).

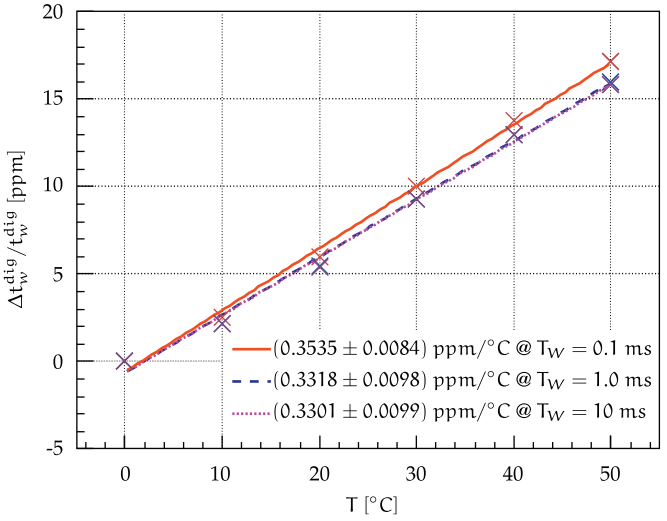

Fig. 4. Pulse width: example of temperature drift trend due to the digital parts (CPLD, Clock-Generator). For all the measured pulse width (100 μs, 0.1 and 10 ms) the resulting trend is compatible.

widths (100 μs, 1 and 10 ms), in order to check also the clock-generator behavior. As shown in Fig. 4, for all the measured widths the temperature trends are linear with (0.33–0.35) ppm/°C slope.

For each temperature we measured also the noise due to the jitter on the width of the output pulses. From Eq. (4) this is given by:

$$\sigma_w = \sqrt{\sigma_w^{dig^2} + \sigma_{12}^2} \quad (6)$$

where σ_w^{dig} and σ_{12} are the distribution variances of the t_w^{dig} and t_{12} measurements, respectively. Results are shown in Table 1. Considering a typical pulse width of $t_w = 1$ ms the noise jitter results to be of the order of about 0.6 ppm, a value much better than the expected detector resolution, which is about 850 ppm (5 KeV_{FWHM} at 2.5 MeV particle energy as a best condition).

Finally, we measured the temperature drift of the pulse amplitude. As given in Eq. (2), its weight is double with respect

Please cite this article as: C. Arnaboldi, et al., Nucl. Instr. and Meth. A (2010), doi:10.1016/j.nima.2010.09.151

Table 1
Resulted noise jitter values. All the values are much better than the expected detector resolution of 850 ppm ($\Delta E \simeq 5$ keV$_{FWHM}$@2.5 MeV).

T (°C)	σ_w^{dig} (ps)	σ_{12} (ps)	σ_w (ps)
0	479.10	203.37	520.48
10	503.79	225.93	552.14
20	525.97	233.05	575.29
30	553.61	236.14	601.87
40	580.78	240.54	628.63
50	616.59	217.29	653.76

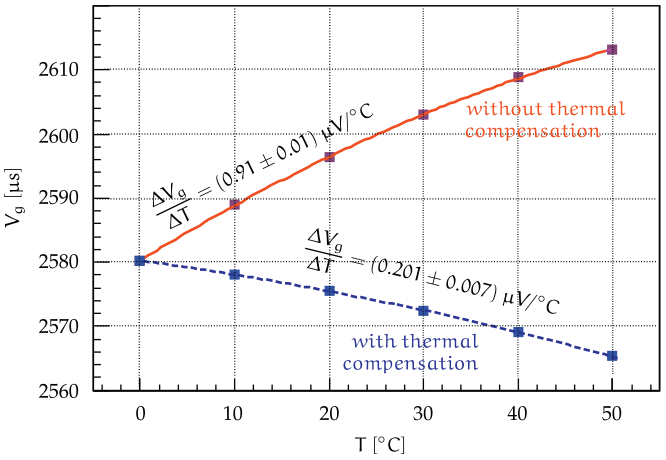

Fig. 5. Pulse amplitude: example of temperature drift trend for a DAC amplitude under 0.625 volts; without (red) and with (blue) thermal gradients suppression. (For interpretation of the references to colour in this figure legend, the reader is referred to the web version of this article.)

to the pulse width, but, on the other hand, it can be compensated exploiting a proper thermal compensation circuit. To characterize the pulse amplitude we used a remote controlled 6-1/2 digits multiplexed multimeter (Keithley® 2700). We performed the measurement for different DAC amplitude values, first without thermal gradients compensation and then introducing it.

The first measurement showed that, for differential amplitudes larger than 0.625 V, the DAC contribution, 2 ppm/°C, is predominant. This drift it is not crucial because it can be compensated exploiting our calibration curves and handling its least significant bits. Below 0.625 V, the main contribution comes from the operational amplifiers. In this case we obtained 0.9 μV/°C (Fig. 5, continuous red line). To compensate this drift we introduced a thermal compensation circuit, as shown in Fig. 6. It works in the following way. Using two calibrated diodes (−1795 μV/°C) and tuning resistors R_1 and R_3, we add to the non-inverting inputs a thermal voltage with a drift equal in magnitude but opposite in sign, with respect to the measured thermal drift at the Op-Amps outputs. After the thermal compensation the drift became 0.2 μV/°C, (Fig. 5, dashed blue line).

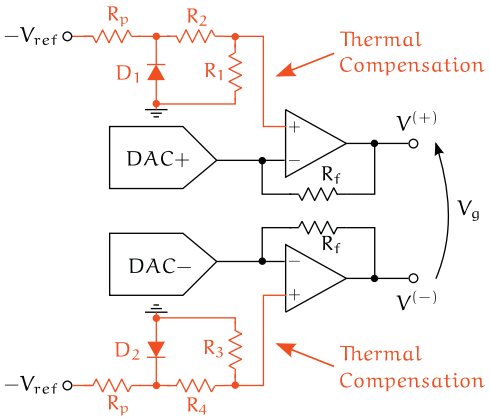

Fig. 6. Simplified scheme of the pulser with the thermal drift calibration system. The networks are connected to the non-inverting input nodes of the Op-Amps.

5. Conclusion

We have realized and characterized the first 4-channels prototype of pulser generator for the CUORE experiment. It is able to generate square pulses having programmable amplitudes and widths. All the features of the realized instrument can be programmed remotely by a message based CAN-Bus protocol.

Characterization results of the pulse width t_w showed that the contribution from the analog part is dominant (2 ppm/°C) in the more stringent condition (100 μs) while at 1 ms, *the typical working condition*, and with larger pulses, the digital contribution becomes prevalent (0.53 ppm/°C in the worst case).

As for the pulse amplitude V_g we have that for settings larger than 1/16 of the full scale, equal to 0.625 V differential, the DACs contribution (2 μV/°C) is predominant (0.2 ppm/°C @ V_g=10 V and 0.8 ppm/°C @ V_g=0.625 V), while for pulse amplitudes below 0.625 V the main contribution is due to the Operational Amplifiers ($\simeq 1$ ppm/°C @ $V_g = 0.625$ V).

References

[1] C. Arnaboldi, et al., Nucl. Instr. and Meth. Phys. Res. A 518 (3) (2004) 775. doi:10.1016/j.nima.2003.07.067, ISSN 0168-9002.
[2] C. Arnaboldi, et al., Phys. Rev. C 78 (3) (2008) 035502. doi:10.1103/PhysRevC.78.035502.
[3] C. Arnaboldi, C. Brofferio, C. Bucci, S. Capelli, O. Cremonesi, E. Fiorini, A. Giuliani, A. Nucciotti, M. Pavan, M. Pedretti, G. Pessina, S. Pirro, C. Pobes, E. Previtali, M. Sisti, M. Vanzini, Phys. Lett. B 557 (3–4) (2003) 167. doi:10.1016/S0370-2693(03)00212-0, ISSN 0370-2693.
[4] A. Alessandrello, C. Brofferio, C. Bucci, O. Cremonesi, A. Giuliani, B. Margesin, A. Nucciotti, M. Pavan, G. Pessina, E. Previtali, M. Zen, Nucl. Instr. and Meth. Phys. Res. A 412 (2–3) (1998) 454. doi:10.1016/S0168-9002(98)00458-6, ISSN 0168-9002.
[5] C. Arnaboldi, G. Pessina, E. Previtali, IEEE Trans. Nucl. Sci. NS-50 (2003) 979. doi:10.1109/TNS.2003.815346.

Please cite this article as: C. Arnaboldi, et al., Nucl. Instr. and Meth. A (2010), doi:10.1016/j.nima.2010.09.151